Published in final edited form as:
Nat Immunol. 2009 November ; 10(11): 1193–1199. doi:10.1038/ni.1789.

CXCL13 is essential for lymph node initiation and is induced by retinoic acid and neuronal stimulation

Serge A. van de Pavert[1], **Brenda J. Olivier**[1,2], **Gera Goverse**[1,2], **Mark F. Vondenhoff**[1,2], **Mascha Greuter**[1], **Patrick Beke**[1], **Kim Kusser**[3], **Uta E. Höpken**[4], **Martin Lipp**[4], **Karen Niederreither**[5], **Rune Blomhoff**[6], **Kasia Sitnik**[7], **William W. Agace**[7], **Troy D. Randall**[3], **Wouter J. de Jonge**[8], and **Reina E. Mebius**[1]

[1]Department of Molecular Cell Biology and Immunology, VU University Medical Center, Amsterdam, the Netherlands [3]Department of Medicine, Division of Allergy, Immunology and Rheumatology, University of Rochester, Rochester, NY 14642, USA [4]Max Delbrück Center for Molecular Medicine, Berlin, Germany [5]Center for Molecular Development and Diseases, Institute of Biosciences and Technology, Texas A&M University, Houston, Texas, USA [6]Faculty of Medicine, Institute of Basic Medical Sciences, University of Oslo, Oslo, Norway [7]Immunology Section, Department of Experimental Medical Science, Lund University, Lund, Sweden [8]Department of Gastroenterology and Hepatology, Academic Medical Center, Amsterdam, The Netherlands

Abstract

Location of embryonic lymph node development is determined by the initial clustering of lymphoid tissue inducer cells. We demonstrate that both CXCL13 and CCL21 attracted E12.5–E14.5 lymphoid tissue inducer cells and that initial clustering exclusively depended on CXCL13. Retinoic acid induced early CXCL13 expression in stromal organizer cells independent of lymphotoxin signaling. Notably, neurons adjacent to the lymph node anlagen expressed enzymes essential for retinoic acid synthesis. Furthermore, stimulation of parasymphathetic neural output in adults led to a retinoic acid receptor-dependent induction of CXCL13 in the gut. Therefore, our data show that initiation of lymph node development is controlled by retinoic acid-mediated expression of CXCL13 and suggest that retinoic acid may be provided by adjacent neurons.

Lymph nodes (LNs) play a central role in the immune system, since they promote efficient interaction of antigen-presenting cells and lymphocytes, increasing the chances that rare antigen-specific lymphocytes become activated. The earliest described steps in LN development involve clustering of hematopoietic lymphoid tissue inducer (LTi) cells with stromal organizer cells1⁻3, followed by the Sengagement of the lymphotoxin-β receptor (LTβR; http://www.signaling-gateway.org/molecule/query?afcsid=A001440) on stromal organizer cells by Lymphotoxin-αβ (L Tαβ; http://www.signaling-gateway.org/molecule/query?afcsid=A001438; http://www.signaling-gateway.org/molecule/query?

Correspondence should be addressed to R.E.M. (R.Mebius@vumc.nl or Tel: +31-20-4448076).
[2]These authors contributed equally

AUTHOR CONTRIBUTIONS

S.A.vd.P., B.O., M.F.V., G.G., M.G., W.J.de.J. and P.B. performed the experiments and data analysis; K.K. and T.R. provided the *Cxcl13*$^{-/-}$ embryos; U.E.H. and M.L. provided the *Cxcr5*$^{-/-}$ embryos; K.N. provided the *Raldh2*$^{-/-}$ embryos; R.B., K.S. and W.W.A. provided the DR5 embryos; S.A.vd.P. and R.E.M. designed the experiments; S.A.vd.P., T.R., and R.E.M. wrote the manuscript; R.E.M. directed the study.

afcsid=A001439)4,5. Embryonic LTi cells in mice are characterized as $CD45^+CD4^+CD3^-\alpha_4\beta_7{}^+$ cells1,6 and require the retinoic orphan receptor RORγt (http://www.signaling-gateway.org/molecule/query?afcsid=A002302) and Id2 for their formation5,7,8, interleukin 7Rα (IL-7Rα; http://www.signaling-gateway.org/molecule/query?afcsid=A001267) for survival and differentiation9,10 and LTαβ for their function4,9. Stromal organizer cells are triggered via LTβR to synthesize chemokines and adhesion molecules that attract and retain more LTi cells11. Lack of LTβR triggering, as seen in mice that lack LTαβ, or LTβR, results in the absence of most LNs12,13. However, clustering of LTi cells during the first stage of LN development is still observed in LTα-deficient mouse embryos5,9,14. The fact that LTi cells cluster independent of LTβR signaling implies that the chemokines that initially attract LTi cells must be induced through other mechanisms.

CXCL13 (http://www.signaling-gateway.org/molecule/query?afcsid=A000378), CCL19 and CCL21 (http://www.signaling-gateway.org/molecule/query?afcsid=A002167) are involved in LTi homing and LN development15,16. Lack of the genes encoding *Ccl21* and *Ccl19*, or their receptor *Ccr7*, does not prevent LN development. However, mice deficient for CXCL13, or its receptor CXCR5 (http://www.signaling-gateway.org/molecule/query?afcsid=A000637), fail to develop peripheral LNs but not the mesenteric, facial or cervical LNs. Only the combined elimination of CXCL13, CCL19 and CCL21, or their receptors, CCR7 (http://www.signaling-gateway.org/molecule/query?afcsid=A000630) and CXCR5, results in absence of most LNs, except the mesenteric LNs16–18. However, the source and function of each individual chemokine during LN development remains unknown.

An analysis of the earliest steps in Peyer's patch development suggests a link between neuronal development and lymphoid organ development. The receptor tyrosine kinase, Ret, which is involved in binding of Glial cell line-derived neurotrophic factor (Gdnf) and is essential for neural crest cell migration and mammalian enteric nervous system formation19, is also required for the migration of $CD11c^+c\text{-}kit^+$ hematopoietic cells that are involved in Peyer's patch formation. Thus, mechanisms that guide nerve fibers may also direct hematopoietic cells to induce Peyer's patch formation.

Retinoic acid (RA) is a vitamin A metabolite that is crucially involved in the development of the nervous system. Lack of Raldh2, the enzyme that metabolizes vitamin A into RA, causes loss of neural crest cell migration20 and enteric neuron development21, 22. RA also plays an important role in several effector functions of the immune system, including immunoglobulin A (IgA) expression by B cells and B cell migration23, induction of chemokine receptors and gut homing molecules on T cells24,25,26 and induction of regulatory T cells (T_{reg}) and T_H-17 cell suppression27. However, the role of RA in LN development is unknown.

Here we show that CXCL13 was crucially involved in the initial clustering of LTi cells and that RA was essential for the early, LTβR-independent expression of CXCL13. Nerve fibers adjacent to CXCL13-expressing stromal organizer cells expressed Raldh2, suggesting that neuronally derived RA led to the expression of CXCL13. In support of this hypothesis, we show that enhancing parasympathetic output activity, by means of efferent vagal nerve stimulation, led to RA receptor dependent induction of CXCL13 in the intestine. Thus, we propose that neuronal production of RA promotes the early, LTβR-independent expression of CXCL13, which in turn leads to the initial clustering of LTi cells and the initiation of LN development.

RESULTS

CXCL13 and CCL21 attract E12.5–E14.5 LTi cells

To study the chemokine responsiveness of LTi cells and their precursors at embryonic days 12 – 14 (E12–E14), we enriched for cells from peripheral LN anlagen by removing all internal organs, including the mesenteric LN and the intestines, and enzymatically digested the remaining embryonic tissue. The resulting single cell suspension was placed in the top chamber of a transwell system and cells were allowed to migrate towards various chemokines, at the determined optimal concentration, located in the bottom chamber. We observed that CXCL13 and CCL21 preferentially attracted $CD4^+CD45^+$ LTi cells (Fig. 1a), corresponding with expression of the responsible receptors CXCR5 and CCR7 on these cells, respectively (Supplementary Fig. 1). A large fraction of the cells that responded to the chemokines expressed intermediate amounts of c-Kit, a hematopoietic stem cell marker and previously used as a marker for the precursor LTi cell population28 (Fig. 1b). In contrast, CXCL12 attracted LTi cells to some extent (20% specific migration, defined as 20% more LTi cells in migrated population when compared to the LTi cell fraction in the original population minus LTi fraction in the auto migration) but also induced chemotaxis of c-Kit^-CD45^+ cells (40% specific migration of c-Kit^-CD45^+ cells compared to original population minus c-Kit^-CD45^+ cells in auto-migrated population) (data not shown). Less than 5% specific migration of hematopoietic cells was observed towards CXCL10 and CCL11 during these stages of LN development (data not shown). These data suggest that CXCL13 and CCL21 preferentially attract LTi cells.

CXCL13 and CCL21 are expressed in early LN anlagen

Since CXCL13 and CCL21 were able to specifically attract (precursor) LTi cells from E12.5–E14.5 LN anlagen, we analyzed the localization of these chemokines during the first phase of LN development. Analysis at E13.5 revealed that CCL21 colocalized with the lymphatic endothelial cell markers, podoplanin (Fig. 2a, arrows), and Lyve-1 (Supplementary Fig. 2a). In contrast, CXCL13 was expressed by $podoplanin^{lo}$ cells that were adjacent to lymphatic endothelial cells (Fig. 2b,c, arrows and (Supplementary Fig. 2b). Importantly, CXCL13 expression was found in all LN anlagen (Fig. 2b–e and Supplementary Fig. 2b–c), while the posterior-located iliac LN anlagen (Fig. 2f and Supplementary Fig. 2d) was still devoid of lymphatic endothelial cells at this stage and hence lacked CCL21 expression. Despite the absence of CCL21 in some LN anlagen at this stage, $CD4^+$ LTi cells still clustered around CXCL13-expressing cells (Fig. 2e,f and Supplementary Fig. 2e). These data suggest that the early expression of CXCL13, and not CCL21, controls the first clustering of LTi cells and thus, the initial development of LNs.

To test the hypothesis that CXCL13 is essential for the first steps in LN development, we examined E14.5 embryos from *Cxcl13*$^{-/-}$ and *Cxcr5*$^{-/-}$ mice. We found that *Cxcl13*$^{-/-}$ E14.5 embryos lacked all LN anlagen (Supplementary Fig. 3a,b), although mesenteric and cervical LN are present in adult mice16,17. Analysis of *Cxcr5*$^{-/-}$ E14.5 embryos confirmed these results, as *Cxcr5*$^{-/-}$ embryos also lacked clusters of LTi cells and LN anlagen (Supplementary Fig. 3c,d). However, a rudimentary mesenteric lymph node was observed in *Cxcr5*$^{-/-}$ mice at E16.5, (Supplementary Fig. 3e). Those data demonstrate that although migration of LTi cells towards CXCL13 is essential for the formation of the initial LTi-stromal cell clusters, the development of mesenteric LNs can be partly rescued during later stages in the absence of CXCR5 (ref. 17).

Since initial clustering of LTi cells occurs independent of LTβR signaling5,9, we reasoned that CXCL13 should be expressed in *Lta*$^{-/-}$ embryos. Indeed, no differences in CXCL13 expression between wild-type and *Lta*$^{-/-}$ mice was observed by real-time PCR in

mesenchymal cells obtained from E12.5–E13 embryos enriched for peripheral LN anlagen (Fig. 3a). Furthermore, CXCL13 was observed within $Lta^{-/-}$ LN anlagen (arrows in Fig. 3b). The staining pattern for CXCL13 in $Lta^{-/-}$ LN anlagen seemed less abundant. Since LTβR triggering may have already taken place in wild-type but not $Lta^{-/-}$ LN anlagen, this signaling might have contributed to CXCL13 protein expression seen in wild-type LN anlagen. These data show that the earliest expression of CXCL13 occurs independently of LTβR signaling.

Retinoic acid induces CXCL13 expression

Since RA is crucial for various developmental processes, we tested whether RA could induce chemokine synthesis in PLN enriched E13.5 mesenchymal cells. While *Cxcl13* expression increased significantly in the RA-treated cells, *Ccl21* expression did not differ between untreated or RA-treated cells (Fig. 4a). The expression of other genes that are regulated via LTβR signaling, such as *Vcam* or *Madcam1* (ref 11, 14, 29), were not increased after RA stimulation (Fig. 4a). Expression of *LTβR* was not affected by RA (data not shown). Moreover, CXCL13 was equally well induced by RA in mesenchymal cells from $Lta^{-/-}$ embryos (Fig. 4b). Thus, these data suggest RA-mediated induction of CXCL13 occurs independently of LTβR signaling. RA regulates gene expression via DNA-binding RA receptors22,30, which act by binding RA responsive elements (RARE) in target genes. In the *Cxcl13* gene we observed several RARE binding sites for RARβ, but not any other RA receptor (Supplementary Table 1). To test whether RARβ was specifically involved in CXCL13 expression, E13.5 mesenchymal cells were stimulated with RA in the presence or absence of the selective RARβ inhibitors, LE540 and LE135 (ref. 31). Incubation of mesenchymal cells with RA greatly induced RARβ mRNA, which was still observed in the presence of the RARβ inhibitors (Fig. 4c). Induction of CXCL13 mRNA by RA, however, was completely prevented by RARβ inhibition (Fig. 4d). Newly translated protein was needed for *Cxcl13* induction, since no increase in CXCL13 mRNA was observed when mesenchymal cells were stimulated with RA in the presence of protein synthesis blocker, cycloheximide, even though RARβ mRNA expression was still induced in the presence of cycloheximide (Fig. 4e). Since CXCL13 induction depends on RARβ, newly formed RARβ is most likely needed for RA mediated induction of CXCL13.

To determine whether RA-induced processes occurred within the LN anlagen *in vivo*, we used DR5-luciferase RARE reporter mouse embryos32. DR5 embryos analyzed at E13.5 and E14.5 had normal appearance of LN anlagen (Fig. 4f). CXCL13-expressing stromal cells within these LN anlagen revealed RARE activation was occurring, as shown by the expression of luciferase (Fig. 4g, arrowheads, and Supplementary Fig. 4).

Retinoic acid is essential for lymph node formation

Given that the induction of CXCL13 depended on the presence of RA and that CXCL13 was crucially involved in the initiation of LN development, then a defect in RA synthesis during embryonic development should result in the lack of LN anlagen. To test this hypothesis, we examined LN anlagen in $Raldh2^{-/-}$ embryos. Since Raldh2 is the most important RA-synthesizing enzyme expressed during embryogenesis, the short-term development of these embryos was rescued through transient RA supplementation at E8.5 (ref. 33,34). Analysis of E13.5 embryos showed that LN anlagen were absent in all embryos analyzed ($n = 5$, not shown). At E14.5 residual LN anlagen containing few $CD4^+$ cells were observed in the axillary region of $Raldh2^{-/-}$ embryos (Supplementary Fig. 5a). In addition, LN anlagen with uncharacteristic localization of Madcam1, Vcam1 and Lyve-1 were detected in the cervical region. In normal cervical LN anlagen Madcam1 was located at the periphery of the cluster of hematopoietic cells, while after LTβR signaling Vcam1 and low amounts of Madcam1 were present on stromal cells within the cluster of hematopoietic cells, and Lyve-1 was

located on the lymph vessels surrounding the LN anlagen. On the contrary, the LN anlagen in the cervical region of *Raldh2*$^{-/-}$ embryos at E14.5 showed that Madcam1 was abundantly present on stromal cells within the anlagen, that Vcam1 was strongly expressed at the border of the anlagen, while Lyve-1 was not expressed on vessels but on single positive cells (Fig. 5a–c and Supplementary Fig. 5b). At both E13.5 and E14.5, most CD4^{+} cells were observed near the dorsal aorta along the whole dorsal side (Supplementary Fig 5b). Almost all CD45^{+} cells within the anlagen in the cervical region (Fig. 5d, arrows) were CD4^{+} and RORγt^{+}, confirming their identity as LTi cells. Expression of lymphatic endothelial cell derived CCL21 was markedly strong within these anlagen (Fig. 5a). As expected, CXCL13 expression was undetectable in most E14.5 *Raldh2*$^{-/-}$ embryos analyzed (Fig. 5b), indicating that Raldh2 and its metabolic product RA were essential for expression of CXCL13 at the start of the LN formation and first LTi cell clustering. Since LTβR triggering can also lead to CXCL13 expression, clustering of LT$\alpha\beta^{+}$CD4^{+} LTi cells near CCL21 expressing lymphatic endothelial cells could subsequently lead to CXCL13 expression as was observed in one occasion in the cervical region of 7 embryos (E13.5–E14.5) analyzed (data not shown). Our data thus support the hypothesis that RA is responsible for the early induction of CXCL13, which attracts the first LTi cells and initiates the formation of LN anlagen. However, in the absence of CXCL13, LTi cells can still respond to CCL21, which is expressed at later times in some locations and may also promote interactions between LTi cells and stromal organizer cells.

Raldh is expressed in adjacent nerve fibers

Having established that RA is crucial for LN development through the induction of CXCL13, we next used immunofluorescence to determine which cells synthesized RA. Immunostaining with antibodies that recognized both Raldh1 and Raldh2 indicated positive structures near all observed LN anlagen (Fig. 6a–d). Staining for Raldh1 or Raldh2 was not observed near LN anlagen in the cervical area of *Raldh2*$^{-/-}$ embryos (data not shown), suggesting that Raldh2, but not Raldh1, was present near LN anlagen. In wild-type embryos, CXCL13 expressing cells could be found directly adjacent to Raldh2-expressing structures (Fig. 6a–c), while Raldh2 was not detectable in either stromal organizer or LTi cells (Fig. 6c). Although CD11c^{+} cells were described to be important for Peyer's patch initiation19 and might thus be a source for RA, we did not observe Raldh in the rare CD11c^{+} cells present in LN anlagen at E13.5 (Supplementary Fig. 6a and data not shown). To determine the cell type that expressed Raldh2, we stained for neuronal markers, including neuronal specific β-III-tubulin (Fig. 6d and Supplementary Fig. 6b–c) and neurofilament (Supplementary Fig. 6d). Notably, Raldh2 co-localized with these neuronal markers near all anlagen, demonstrating that neurons express Raldh2 and are a potential source of RA.

Vagal nerve stimulation leads to CXCL13 expression

The vagal nerve innervates the intestines and the stimulation of vagal efferent output can affect the mucosal immune system35. Thus, to further address whether neurons could induce CXCL13 expression in neighboring mesenchymal cells, we tested the effect of electrical stimulation of the right cervical vagal nerve36 on CXCL13 expression in the ileum. First we determined the optimal time for induction of CXCL13 in the ileum at 4, 8 and 24 h after stimulation. We observed that CXCL13 was significantly induced at 8 h (Fig. 7a). Subsequently, we tested whether CXCL13 induction at 8 h after stimulation required RARβ by administering the RARβ inhibitors, LE540 and LE135, intraperitoneally 30 min before vagal nerve stimulation. We found that blocking RARβ abolished the induction of CXCL13 (Fig. 7b). Thus, vagal nerve stimulation leads to the RARβ-dependent induction of CXCL13.

DISCUSSION

The current paradigm of LN development suggests that the first step in this process is the clustering of LTi and stromal organizer cells at site of LN formation5,9,14, followed by the engagement of LTβR on stromal organizer cells, which leads to enhanced expression of homeostatic chemokines and eventual recruitment of lymphocytes (reviewed in2). However, for the initial attraction of LTi cells, one or more of the homeostatic chemokines must be expressed in the developing LN anlagen prior to the engagement of the LTβR by LTαβ on LTi cells. Here we show that although both CXCL13 and CCL21 potently attract LTi cells from day E12.5–14.5 embryos, only CXCL13 was expressed in all LN anlagen at this time. As predicted, the early expression of CXCL13 occurred independently of LTβR signaling. Instead, we found that RA induced CXCL13 expression in mesenchymal cells and that early CXCL13 expression was abrogated in mice lacking the RA-synthesizing enzyme, Raldh2. Importantly, all LN anlagen were lacking in E14.5 *Cxcr5*$^{-/-}$ and *Cxcl13*$^{-/-}$ embryos and were either missing or aberrantly formed in *Raldh2*$^{-/-}$ mice. Thus, we conclude that the early, RA-dependent expression of CXCL13 is essential for the initial attraction of LTi cells and the formation of the early LN anlagen.

Although the initial formation of the LN anlagen was dependent on CXCL13, some LNs do develop in *Cxcl13*$^{-/-}$ and *Cxcr5*$^{-/-}$ mice16,17,37, probably due to the recruitment of LTi cells by CCL21 that is expressed at later times by lymphatic endothelial cells. Consistent with this conclusion, cervical LNs do not develop in *Cxcr5*$^{-/-}$ × *Ccr7*$^{-/-}$ mice18, which lack the ability to respond to either CXCL13 or CCL21. However, they do develop in *Plt* × *Cxcl13*$^{-/-}$ mice16, which still retain CCL21 expression on lymphatic endothelial cells. The formation of abnormal LN anlagen in the cervical area of *Raldh2*$^{-/-}$ embryos at E14.5 is also in agreement with this conclusion, since CCL21, but not CXCL13, is expressed in the cervical LN anlagen of *Raldh2*$^{-/-}$ mice. As a result, LTi cells are initially recruited to the anlagen of cervical LNs by CCL21 and then interactions between LTi cells and stromal organizer cells allow LTβR-signaling, resulting in cervical LN formation. In the case of the MLNs, lack of CXCL13, or its receptor, can be rescued by unknown agents after E14.5 and before E16.5, since we observed a rudimentary MLN at E16.5 in the *Cxcr5*$^{-/-}$ mice. This rescue occurs around the time of Peyer's patch formation, indicating that these processes might share common initiation cues. Unfortunately, embryos lacking *Raldh2* die well before E16.5 making this mouse model unfit to analyze the role for RA in the formation of MLNs or Peyer's patches.

It has been suggested that the nervous system regulates lymphoid organogenesis during Peyer's patch formation19, since the cells that initiate Peyer's patch development follow the migratory cues that are essential for the development of the enteric nervous system. Another example of neuronal influence on the immune system is the immune modulating effect of the nervus vagus (reviewed in 38,39). We show that vagal nerve stimulation causes the induction of CXCL13 in adult intestines and that this process also depends on RA receptor signaling, although an indirect effect of the stimulated vagal nerve on induction of CXCL13 cannot be ruled out. Similarly, initial expression of CXCL13 during lymph node development depends on RA and may involve neurons that are positioned directly adjacent to CXCL13 expressing cells. Although we could not detect RALDH protein on mesenchymal or hematopoieitic cells in lymph node anlagen between E12.5 and E14.5, low amounts may be present and further contribute to CXCL13 expression. We propose that during the initiation of lymph node development neuronal derived RA induces CXCL13 expression in mesenchymal cells and that this process determines the location of lymph nodes by attraction of the first LTi cells. The mechanism by which RA is transferred to adjacent cells is unknown, but other paracrine effects of RA in the immune system have been described before24,25. Obviously, LNs are not formed along the entire neuron,

whereas Raldh2 is expressed throughout the nerve fiber. We have observed that LN anlagen are often formed at the location where blood vessels branch (unpublished observations). These locations may somehow instruct nerve fibers to release RA. The exact mechanism that determines the location of RA release will require further studies.

Our findings might further explain the numerous reports of CXCL13 expression and B cell follicles at sites of chronic inflammation or rejection[40–44]. In analogy with our findings on LN formation, we propose that neuronal-derived RA at these sites of inflammation might similarly act on stromal cells to induce CXCL13 expression, leading to the attraction of B cells. Indeed, an increase in nerve fibers has been reported at sites of chronic inflammation[45,46], most likely due to the expression of neurotrophic factors[45,47]. Expression of CXCL13 at the earliest stage of the development of rheumatoid synovitis, before the detection of any organized B cell cluster, has been reported[48]. Furthermore, the induced expression of CXCL13 in the lungs after influenza infection occurs independently of LTα[49], suggesting that other mechanisms, such as the induction of CXCL13 by RA, might play a role in the formation of ectopic follicles in the lung. The presented findings provide evidence that CXCL13 and RA are indispensable for the clustering of LTi cells during the first phase of lymph node formation and factors in the RA-CXCL13-CXCR5 axis may similarly be important in the initiation of ectopic lymphoid structures during chronic inflammation.

METHODS

Animals

C57BL/6 mice, *Lta*$^{-/-}$, *Cxcr5*$^{-/-}$ *Cxcl13*$^{-/-}$ *Raldh2*$^{-/-}$ and DR5-RARE luciferase mice were described before[17,29,32,33,37]. Embryos were fixed for 30 min in 4% formalin or paraformaldehyde in PBS, cryoprotected overnight in 30% sucrose in PBS and stored in OCT embedding medium at −80 °C. For electrical vagal nerve stimulation, 12 to 15 week-old female BALB/c mice (Harlan Nederland) were kept under environmentally controlled conditions (light on from 8:00 AM till 8:00 PM; water and rodent non-purified diet *ad libitum*; temperature 20–22 °C; 55% humidity). All animal experiments were approved by the local animal experimental committees.

Immunofluorescence, flow cytometry and qPCR

For identification of LN anlagen embryos were serially sectioned and every 10th section was stained with anti-Madcam1, CD4 and CD45. Adjacent sections containing LN anlagen were used for further analysis. Stainings and FACS analysis were performed as previously described[11]. QPCR primers are shown in Supplementary Table 2 and cDNA or PCR reactions were carried out as previously described[11]. 8 μm Cryosections were dehydrated in acetone for 10 min and air-dried for an additional 10 min. Biotinyated anti-CXCL13 and anti-CCL21 (R&D systems) were visualized with a TSA signal amplification Kit with HRP-streptavidin and Alexa Fluor 546 tyramide (Invitrogen). To assure antibody specificity, isotype controls were used as replacement of the primary incubation. Sections were analyzed on a Leica TCS SP2 confocal laser-scanning microscope (Leica Microsystems) and Photoshop (CS3, Adobe). Flow cytometric analyses were performed using a Cyan (Beckman Coulter), and Summit software (v4.3, Beckman Coulter).

Antibodies

8.1.1 (anti-podoplanin), hamster monoclonal anti-RORγ, GK1.5 (anti-CD4), MECA-367 (anti-mucosal addressin cell adhesion molecule-1 (Madcam1)), MP33 (anti-CD45) and A7R34 (anti-IL7Rα) were affinity purified from hybridoma cell culture supernatants with protein G-Sepharose (Pharmacia) and labeled with Alexa-Fluor 488 or Alexa-Fluor 647

(Invitrogen). 2B8 was directly labeld to PE (anti-c-Kit) (BD Biosciences). 2G8-biotin (anti-CXCR5) (BD Biosciences) was visualized with streptadivin-Alexa-Fluor 647 (Invitrogen). TG8 (anti-CCR7) (Biolegend) was directly labeled to Alexa-Fluor 647. 429 (anti-Vcam1) (BD Biosciences), anti-Lyve1 (Millipore), anti-neurofilament 200 (Sigma), TUJ-1 (neuron specific beta III Tubulin antibody, Abcam), anti-Raldh1/2 (Abcam, catalog number ab23375) and anti-luciferase (Abcam and Millipore) were used as unconjugated primary antibodies. Mono- or polyclonal antibodies were visualized with Alexa-Fluor 488, Alexa-Fluor 546 or Alexa-Fluor 647-conjugated anti-rat IgG, anti-mouse IgG, anti-Syrian hamster IgG, anti-rabbit IgG, anti-goat IgG (Invitrogen) or Cy3-conjugated goat anti-Armanian hamster (Jackson Immuno Research Laboratory) as appropriate.

Ex vivo cell culture and chemokine migration assay

From E12–E14 embryos the anterior part of the head, extremities and organs (including all hematopoietic cell containing organs and MLN) were removed. The remaining tissue was brought into cell suspension with 0.5 mg/ml Blenzyme 2 (Roche), 0.2 mg/ml DNaseI (Roche) in PBS for 15 min at 37 °C while stirring. Cell suspensions were washed with RPMI (Invitrogen), supplemented with 2% heat-inactivated FCS, 100 U/ml penicillin, and 100 μg/ml streptomycin. Cells were either directly used for FACS analysis of CXCR5 and CCR7 expression or allowed to adhere for 2 h at 37 °C to enrich for the non-adhering hematopoietic cells, which were subsequently used in chemokine assays as previously described50. In short, 5.0×10^5 non-adhering cells were transferred to a transwell with 5.0 μm pore size (Corning). In the bottom well chemokines were added ranging from 0.01 to 5 μg/ml. Concentrations optimal for chemotaxis were determined to be 0.1 μg/ml for CXCL12 and 1 μg/ml for CXCL13 and CCL21. After 3 h incubation at 37 °C and 5% CO_2, cells from the bottom well were harvested, counted and stained with anti c-Kit, CD4 and CD45. Dead cells were gated out using Sytox blue (Invitrogen). Specific migration was calculated using the following formula: % specific migration= [((total amount migrated cells × percentage of gated migrated cells) - (total amount automigrated cells × percentage of gated automigrated cells)) / (total amount of original population × percentage of gated orginal population)] × 100 %.

For RA stimulation experiments, RA (dissolved as 10 mM in 100% ethanol) was added to adherent cells at 100 nM while untreated cells received vehicle alone. Cycloheximide (dissolved in PBS)(Sigma) was added at 10 μg/ml 1 h prior to RA stimulation. RARβ inhibitors LE540 (Wako chemicals) and LE135 (Tocris Biosciences) (both dissolved in 100% ethanol at 10 mM) were added at 10 μM, of which half was added at 30 min prior to RA addition and the other half at the moment of RA stimulation. After 6 h incubation at 37 °C and 5% CO_2, adhered cells were harvested in Trizol (Sigma) and RNA isolated using manufacturer's protocol.

Electrical vagal nerve stimulation

Mice were anesthetized by i.p. injection of a mixture of Fentanyl Citrate / Fluanisone (Hypnorm; Janssen) and Midazolam (Dormicum; Roche). VNS was performed as described previously35. In short: the right cervical vagal branch was prepared free from the carotid artery and ligated with 6-0 silk suture. The distal part from the ligation was attached to a bipolar electrode and 5 V stimuli with a frequency of 5 Hz, duration of 2 ms were applied for 15 min. In sham operated mice the cervical skin was opened and left for 15 min covered by moist gauze. To determine optimal stimulation protocol, groups of 3 animals were electrically stimulated and ileum was collected at 4, 8 and 24 h after stimulation. For RARβ blocking, LE135 and LE540 were administered 30 min prior to VNS. LE135 and LE540 were dissolved at 10 mM in 100% ethanol, of which 100 μg was injected in 200 μl PBS intraperitoneally (ip), as was described before26. As control, vehicle was injected ip. After 8

h, ileum was snap frozen and stored at −80 °C until subsequent RNA isolation, by homogenization in Trizol, using manufactures protocol. The group of 3 animals that had each received either sham or electrical stimulation in the optimalization experiment, but which had received no ip injection, were not statistically significantly different from their vehicle ip injected counterparts and were consequently incorporated in the group.

Statistical Analysis

All analysis were performed by a two-tailed unpaired Student T-test against RA unstimulated cells, statistically significant P values are provided in the figures.

Supplementary Material

Refer to Web version on PubMed Central for supplementary material.

Acknowledgments

Animal caretakers for their care of the animals. G. Kraal and T. Geijtenbeek for critically reading the manuscript, R. Molenaar for help and H. Kalay for labeling of the antibodies. D. Littman (Skirball Institute of Biomolecular Medicine, USA), S. Nishikawa (Riken Center for Developmental Biology, Japan) and K. van Gisbergen (AMC, the Netherlands) for providing antibodies. J. van der Meulen (CBS, the Netherlands) for her help in the statistical analysis. This work was supported by NIH grants (HL69409 and AI072689) (T.D.R.), a VIDI (016.096.310) (W.J.dJ), and VICI grant (918.56.612) (R.E.M and S.A.vd.P.) and a Genomics grant (050-10-120) (R.E.M. and M.F.V.) from the Netherlands Organization for Scientific Research.

References

1. Mebius RE, Streeter PR, Michie S, Butcher EC, Weissman IL. A developmental switch in lymphocyte homing receptor and endothelial vascular addressin expression regulates lymphocyte homing and permits $CD4^+CD3^-$ cells to colonize lymph nodes. Proc. Natl. Acad. Sci. USA. 1996; 93:11019–11024. [PubMed: 8855301]
2. Mebius RE. Organogenesis of lymphoid tissues. Nat. Rev. Immunol. 2003; 3:292–303. [PubMed: 12669020]
3. Cupedo T, Mebius RE. Cellular interactions in lymph node development. J Immunol. 2005; 174:21–25. [PubMed: 15611222]
4. Yoshida H, et al. Expression of $\alpha_4\beta_7$ Integrin Defines a Distinct Pathway of Lymphoid Progenitors Committed to T Cells, Fetal Intestinal Lymphotoxin Producer, NK, and Dendritic Cells. J Immunol. 2001; 167:2511–2521. [PubMed: 11509590]
5. Eberl G, et al. An essential function for the nuclear receptor RORγt in the generation of fetal lymphoid tissue inducer cells. Nat Immunol. 2004; 5:64–73. [PubMed: 14691482]
6. Mebius RE, Rennert P, Weissman IL. Developing Lymph Nodes Collect $CD4^+CD3^-$ $LT\beta^+$ Cells That Can Differentiate to APC, NK Cells, and Follicular Cells but Not T or B Cells. Immunity. 1997; 7:493–504. [PubMed: 9354470]
7. Sun Z, et al. Requirement for RORγ in Thymocyte Survival and Lymphoid Organ Development. Science. 2000; 288:2369–2373. [PubMed: 10875923]
8. Boos MD, Yokota Y, Eberl G, Kee BL. Mature natural killer cell and lymphoid tissue-inducing cell development requires Id2-mediated suppression of E protein activity. J Exp. Med. 2007; 204:1119–1130. [PubMed: 17452521]
9. Yoshida H, et al. Different Cytokines Induce Surface Lymphotoxin–αβ on IL–7 Receptor–α Cells that Differentially Engender Lymph Nodes and Peyer's Patches. Immunity. 2002; 17:823–833. [PubMed: 12479827]
10. Meier D, et al. Ectopic Lymphoid–Organ Development Occurs through Interleukin 7–Mediated Enhanced Survival of Lymphoid–Tissue–Inducer Cells. Immunity. 2007; 26:643–654. [PubMed: 17521585]
11. Cupedo T, et al. Presumptive lymph node organizers are differentially represented in developing mesenteric and peripheral nodes. J Immunol. 2004; 173:2968–2975. [PubMed: 15322155]

12. De Togni P, et al. Abnormal development of peripheral lymphoid organs in mice deficient in lymphotoxin. Science. 1994; 264:703–707. [PubMed: 8171322]
13. Rennert PD, James D, Mackay F, Browning JL, Hochman PS. Lymph Node Genesis Is Induced by Signaling through the Lymphotoxin β Receptor. Immunity. 1998; 9:71–79. [PubMed: 9697837]
14. Vondenhoff MF, et al. LTbetaR signaling induces cytokine expression and up–regulates lymphangiogenic factors in lymph node anlagen. J Immunol. 2009; 182:5439–5445. [PubMed: 19380791]
15. Luther SA, et al. Differing activities of homeostatic chemokines CCL19, CCL21, and CXCL12 in lymphocyte and dendritic cell recruitment and lymphoid neogenesis. J Immunol. 2002; 169:424–433. [PubMed: 12077273]
16. Luther SA, Ansel KM, Cyster JG. Overlapping Roles of CXCL13, Interleukin 7 Receptor α and CCR7 Ligands in Lymph Node Development. J. Exp. Med. 2003; 197:1191–1198. [PubMed: 12732660]
17. Ansel KM, et al. A chemokine–driven positive feedback loop organizes lymphoid follicles. Nature. 2000; 406:309–314. [PubMed: 10917533]
18. Ohl L, et al. Cooperating mechanisms of CXCR5 and CCR7 in development and organization of secondary lymphoid organs. J Exp. Med. 2003; 197:1199–1204. [PubMed: 12732661]
19. Veiga–Fernandes H, et al. Tyrosine kinase receptor RET is a key regulator of Peyer's patch organogenesis. Nature. 2007; 446:547–551. [PubMed: 17322904]
20. Niederreither K, et al. The regional pattern of retinoic acid synthesis by RALDH2 is essential for the development of posterior pharyngeal arches and the enteric nervous system. Development. 2003; 130:2525–2534. [PubMed: 12702665]
21. Vermot J, et al. Retinaldehyde dehydrogenase 2 and Hoxc8 are required in the murine brachial spinal cord for the specification of Lim1+ motoneurons and the correct distribution of Islet1+ motoneurons. Development. 2005; 132:1611–1621. [PubMed: 15753214]
22. Niederreither K, Dolle P. Retinoic acid in development: towards an integrated view. Nat Rev. Genet. 2008; 9:541–553. [PubMed: 18542081]
23. Mora JR, et al. Generation of gut–homing IgA–secreting B cells by intestinal dendritic cells. Science. 2006; 314:1157–1160. [PubMed: 17110582]
24. Johansson–Lindbom B, Agace WW. Generation of gut–homing T cells and their localization to the small intestinal mucosa. Immunol Rev. 2007; 215:226–242. [PubMed: 17291292]
25. Mebius RE. Vitamins in control of lymphocyte migration. Nat Immunol. 2007; 8:229–230. [PubMed: 17304229]
26. Hammerschmidt SI, et al. Stromal mesenteric lymph node cells are essential for the generation of gut–homing T cells in vivo. J Exp. Med. 2008; 205:2483–2490. [PubMed: 18852290]
27. Mucida D, et al. Reciprocal T_H17 and regulatory T cell differentiation mediated by retinoic acid. Science. 2007; 317:256–260. [PubMed: 17569825]
28. Mebius RE, et al. The fetal liver counterpart of adult common lymphoid progenitors gives rise to all lymphoid lineages, $CD45^+CD4^+CD3^-$ cells, as well as macrophages. J Immunol. 2001; 166:6593–6601. [PubMed: 11359812]
29. Vondenhoff MF, et al. Separation of splenic red and white pulp occurs before birth in a LTαβ–independent manner. J Leukoc. Biol. 2008; 84:152–161. [PubMed: 18403646]
30. Schug TT, Berry DC, Shaw NS, Travis SN, Noy N. Opposing Effects of Retinoic Acid on Cell Growth Result from Alternate Activation of Two Different Nuclear Receptors. Cell. 2007; 129:723–733. [PubMed: 17512406]
31. Li Y, Hashimoto Y, Agadir A, Kagechika H, Zhang X. Identification of a novel class of retinoic acid receptorβ–selective retinoid antagonists and their inhibitory effects on AP–1 activity and retinoic acid–induced apoptosis in human breast cancer cells. J Biol Chem. 1999; 274:15360–15366. [PubMed: 10336422]
32. Svensson M, et al. Retinoic acid receptor signaling levels and antigen dose regulate gut homing receptor expression on $CD8^+$ T cells. Mucosal Immunol. 2008; 1:38–48. [PubMed: 19079159]
33. Niederreither K, Subbarayan V, Dolle P, Chambon P. Embryonic retinoic acid synthesis is essential for early mouse post–implantation development. Nat Genet. 1999; 21:444–448. [PubMed: 10192400]

34. Niederreither K, et al. Embryonic retinoic acid synthesis is essential for heart morphogenesis in the mouse. Development. 2001; 128:1019–1031. [PubMed: 11245568]
35. de Jonge WJ, et al. Stimulation of the vagus nerve attenuates macrophage activation by activating the Jak2–STAT3 signaling pathway. Nat Immunol. 2005; 6:844–851. [PubMed: 16025117]
36. Borovikova LV, et al. Vagus nerve stimulation attenuates the systemic inflammatory response to endotoxin. Nature. 2000; 405:458–462. [PubMed: 10839541]
37. Forster R, et al. A putative chemokine receptor, BLR1, directs B cell migration to defined lymphoid organs and specific anatomic compartments of the spleen. Cell. 1996; 87:1037–1047. [PubMed: 8978608]
38. Van Der Zanden EP, Boeckxstaens GE, de Jonge WJ. The vagus nerve as a modulator of intestinal inflammation. Neurogastroenterol. Motil. 2009; 21:6–17. [PubMed: 19140954]
39. Tracey KJ. Physiology and immunology of the cholinergic antiinflammatory pathway. J Clin. Invest. 2007; 117:289–296. [PubMed: 17273548]
40. Magliozzi R, Columba–Cabezas S, Serafini B, Aloisi F. Intracerebral expression of CXCL13 and BAFF is accompanied by formation of lymphoid follicle–like structures in the meninges of mice with relapsing experimental autoimmune encephalomyelitis. J Neuroimmunol. 2004; 148:11–23. [PubMed: 14975582]
41. Wengner AM, et al. CXCR5– and CCR7–dependent lymphoid neogenesis in a murine model of chronic antigen–induced arthritis. Arthritis Rheum. 2007; 56:3271–3283. [PubMed: 17907173]
42. Meraouna A, et al. The chemokine CXCL13 is a key molecule in autoimmune myasthenia gravis. Blood. 2006; 108:432–440. [PubMed: 16543475]
43. Steinmetz OM, et al. BCA–1/CXCL13 expression is associated with CXCR5–positive B–cell cluster formation in acute renal transplant rejection. Kidney Int. 2005; 67:1616–1621. [PubMed: 15780119]
44. Bagaeva LV, Rao P, Powers JM, Segal BM. CXC chemokine ligand 13 plays a role in experimental autoimmune encephalomyelitis. J Immunol. 2006; 176:7676–7685. [PubMed: 16751415]
45. Grimsholm O, Guo Y, Ny T, Forsgren S. Expression patterns of neurotrophins and neurotrophin receptors in articular chondrocytes and inflammatory infiltrates in knee joint arthritis. Cells Tissues. Organs. 2008; 188:299–309. [PubMed: 18349525]
46. Sugiura H, Omoto M, Hirota Y, Danno K, Uehara M. Density and fine structure of peripheral nerves in various skin lesions of atopic dermatitis. Arch. Dermatol. Res. 1997; 289:125–131. [PubMed: 9128759]
47. Batchelor PE, Wills TE, Hewa AP, Porritt MJ, Howells DW. Stimulation of axonal sprouting by trophic factors immobilized within the wound core. Brain Res. 2008; 1209:49–56. [PubMed: 18396265]
48. Manzo A, et al. Systematic microanatomical analysis of CXCL13 and CCL21 in situ production and progressive lymphoid organization in rheumatoid synovitis. Eur. J Immunol. 2005; 35:1347–1359. [PubMed: 15832291]
49. Moyron–Quiroz JE, et al. Role of inducible bronchus associated lymphoid tissue (iBALT) in respiratory immunity. Nat Med. 2004; 10:927–934. [PubMed: 15311275]
50. Cupedo T, et al. Initiation of cellular organization in lymph nodes is regulated by non–B cell–derived signals and is not dependent on CXC chemokine ligand 13. J Immunol. 2004; 173:4889–4896. [PubMed: 15470030]

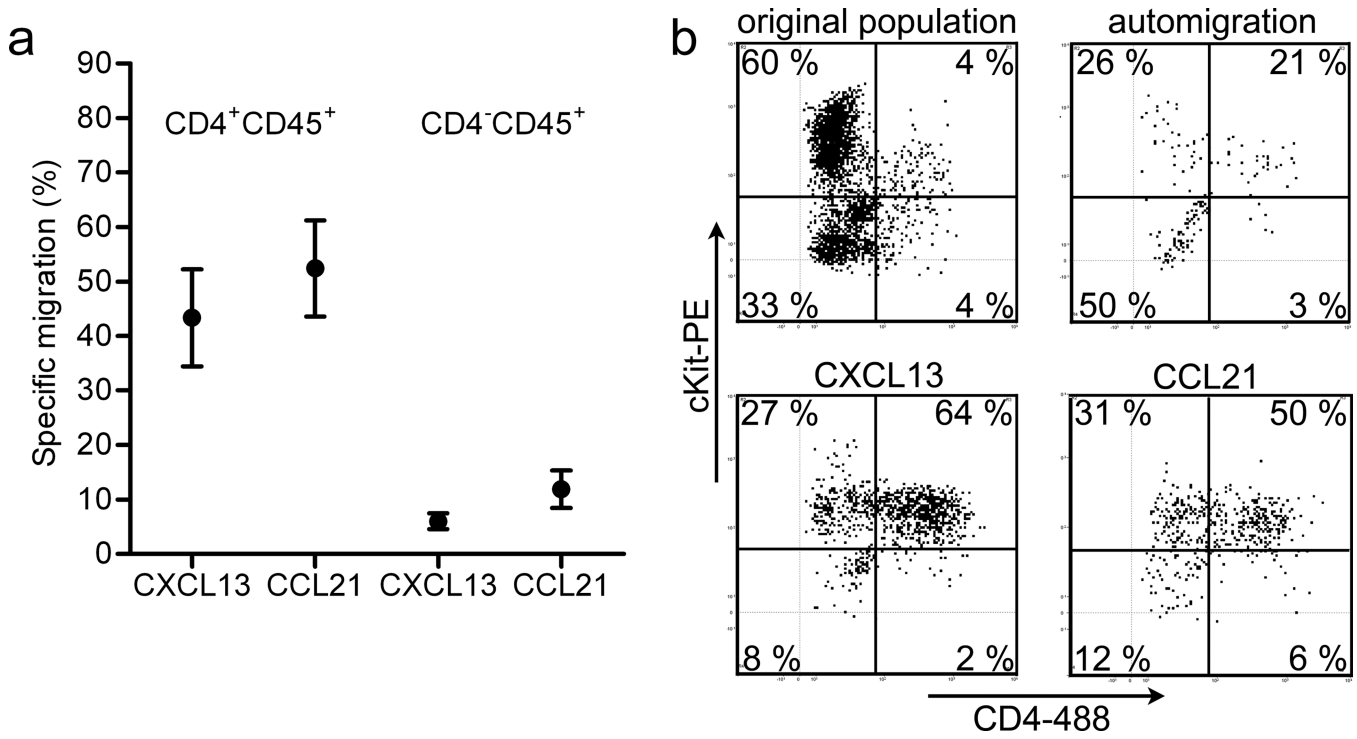

Figure 1. Specific migration of LTi cells and precursors towards chemokines

(**a**) Averaged specific migration values of cell populations from E12.5–14.5 ($n = 8$ independent experiments with each containing at least 8 embryos). $CD4^+CD45^+$ represent LTi cells. Error bars in the graph represent the standard error. (**b**) Representative FACS analysis (of 8 independent experiments) of hematopoietic cells that responded to the indicated chemokine. Cells were additionally stained for c-Kit and CD4, allowing identification of LTi precursor cells ($c\text{-}Kit^+CD4^-$) and LTi cells ($c\text{-}Kit^+CD4^+$).

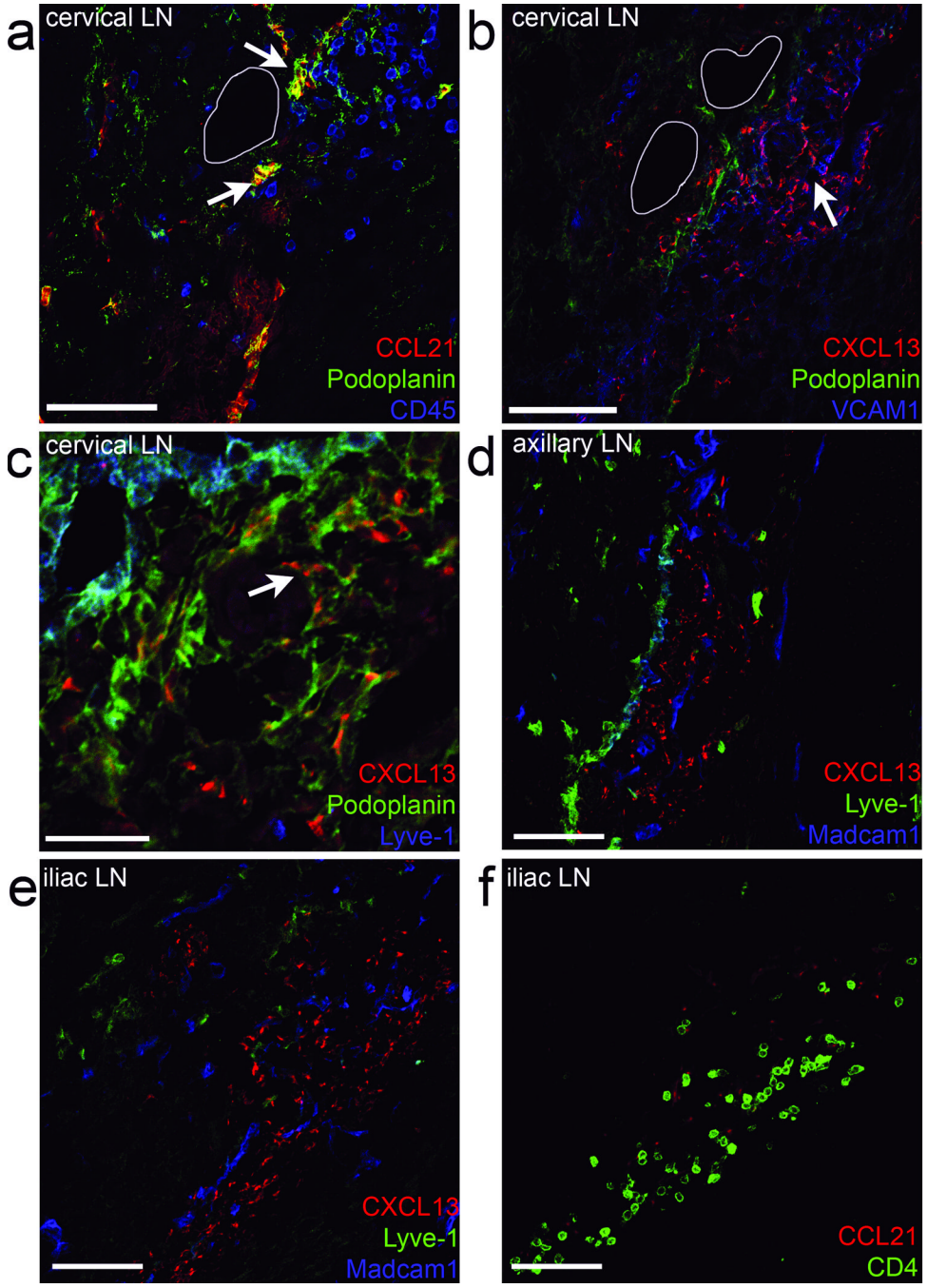

Figure 2. Chemokines CXCL13 and CCL21 are present in E13.5 developing lymph nodes

Embryonic LN anlagen ($n = 8$) were first identified by Madcam1 and CD4 localization. (**a**) The cervical LN anlagen was stained for chemokines CCL21 (arrow in **a**) and CXCL13 in a subsequent section (**b**). (**c**) A highly magnified area of the cervical LN shown in (**a–b**) stained for CXCL13. (**a**) To identify hematopoietic cells within the anlagen, CD45 was used. (**a–c**). To identify stromal organizer and lymphatic endothelial cells, Podoplanin was used. (**c–e**) Lymphatic endothelial cells are identified as Lyve-1^{+} and Podoplanin^{high}, while stromal organizer cells are Podoplanin^{+} and VCAM1^{+} (**b**). The white lines represent blood vessels (**a–b**). (**d–e**) Also other LN anlagen, such as the axillary or more posterior located

iliac LN, were stained for CXCL13, Madcam1, and Lyve-1. (**f**) The subsequent section of the iliac LN anlagen, was stained for Lyve-1, Ccl21, and CD4. Bars represent 25 μm in c and 75 μm in others.

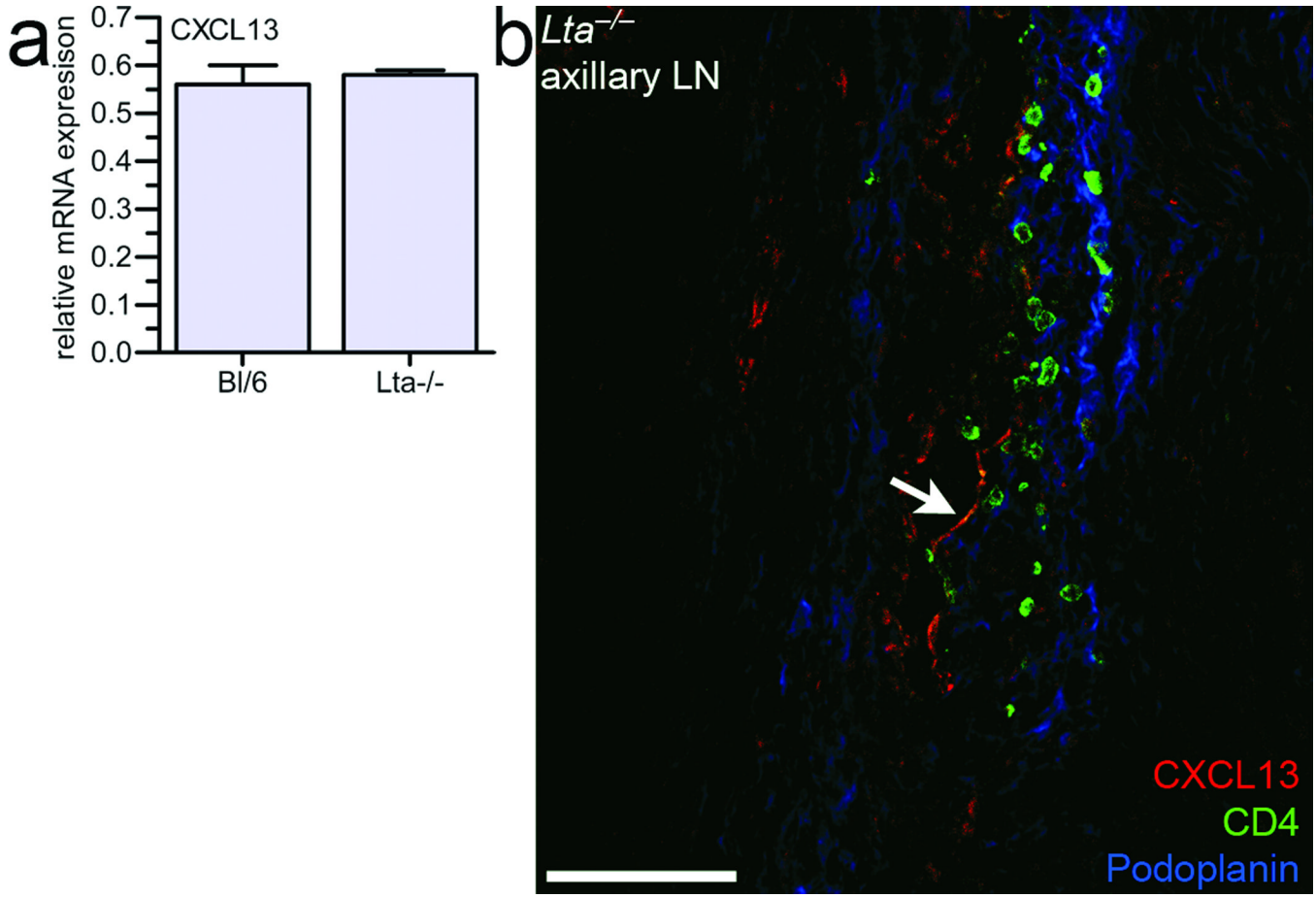

Figure 3. LN development and CXCL13 expression occur independent of LTβR signaling

(**a**) mRNA levels of CXCL13 were measured in E12.5–E13 *Lta*$^{-/-}$ and wild type embryonic mesenchymal cells ($n = 4$). (**b**) Embryonic LN anlagen from E14.5 *Lta*$^{-/-}$ were stained for CXCL13 (arrow), CD4, and Podoplanin. Bar represents 75 μm.

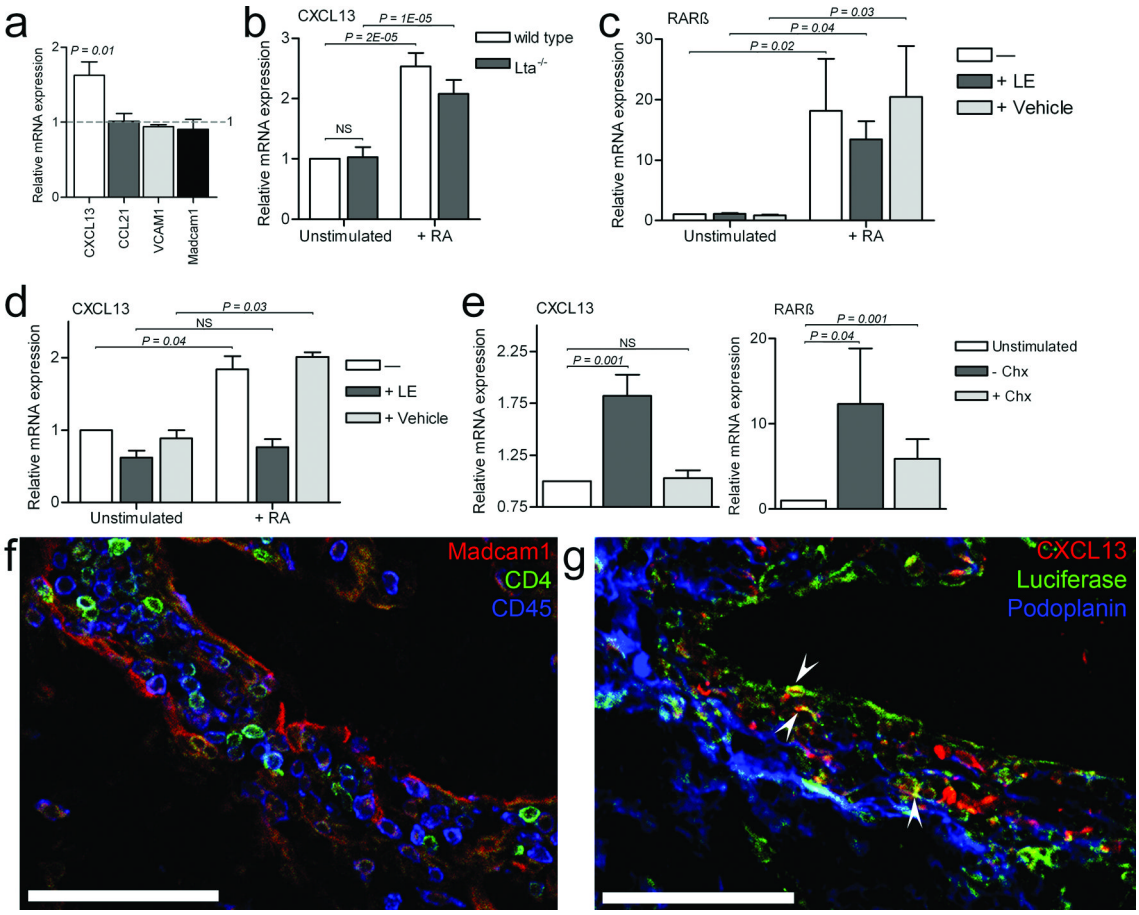

Figure 4. Retinoic acid induces the expression of chemokine CXCL13 via RARβ

(**a**) CXCL13, CCL21, VCAM1, and Madcam1 mRNA in E13.5 Bl/6 embryonic cells in the presence of RA for 6h compared to untreated cells ($n = 5$). (**b**) CXCL13 mRNA in unstimulated mesenchymal cells from E12.5–E13.5 $Lta^{-/-}$ and Bl/6 wild type embryos ($n = 7$) and after RA treatment. (**c**) RARβ or (**d**) CXCL13 mRNA in unstimulated mesenchymal cells from E13.5 Bl/6 wild type embryos and after RA treatment ($n = 5$), in the presence (+LE) or absence (vehicle) of specific RARβ inhibitors LE540 and LE135 (LE). (**e**) CXCL13 or RARβ mRNA in unstimulated mesenchymal cells from E13.5 Bl/6 wild type embryos, after RA treatment ($n = 8$), and after RA treatment in the presence of cycloheximide (Chx). Error bars represent the standard error. NS means not statistically significant ($P > 0.05$). (**f–g**) Cervical LN anlagen in E14.5 DR5-luciferase embryo ($n = 4$) stained for (**f**) Madcam1, CD4, CD45, or (**g**) podoplanin, Cxcl13, and luciferase (arrowheads). Bars represent 75 μm.

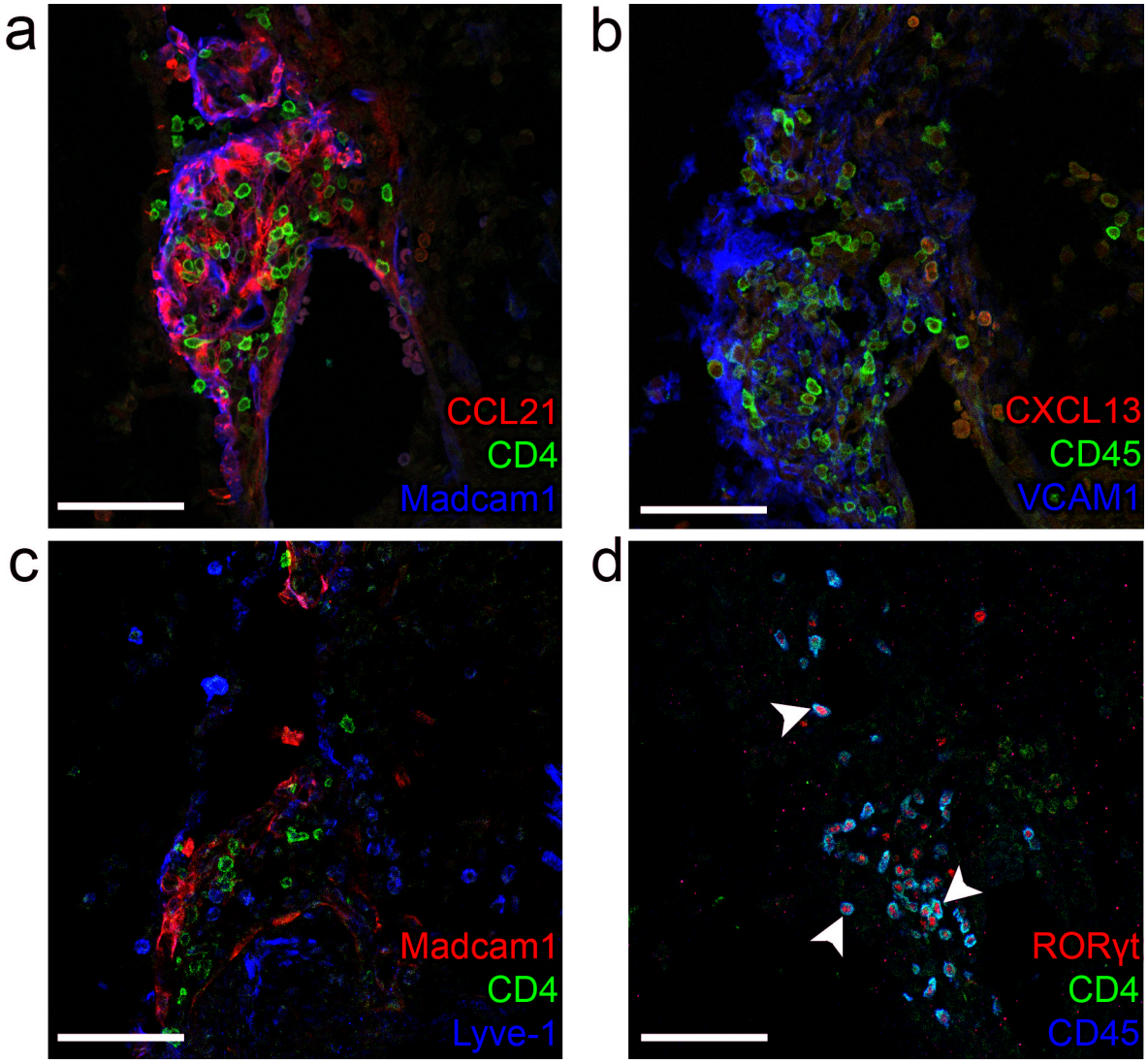

Figure 5. Most LN anlagen are lacking in *Raldh2*$^{-/-}$ E14.5 embryos

In *Raldh2*$^{-/-}$ embryos at E14.5 ($n = 3$), serial sections of LN anlagen in the cervical area were stained for CCL21, CD4 and Madcam1 (**a**), and CXCL13, CD45 and VCAM1 (**b**). (**c**) Anti-Lyve-1 was used to stain lymphatic endothelial cells. (**d**) LTi cells were stained with anti-CD45, anti-CD4 and anti-RORγt (arrowheads in **d**). Bars represent 75 μm.

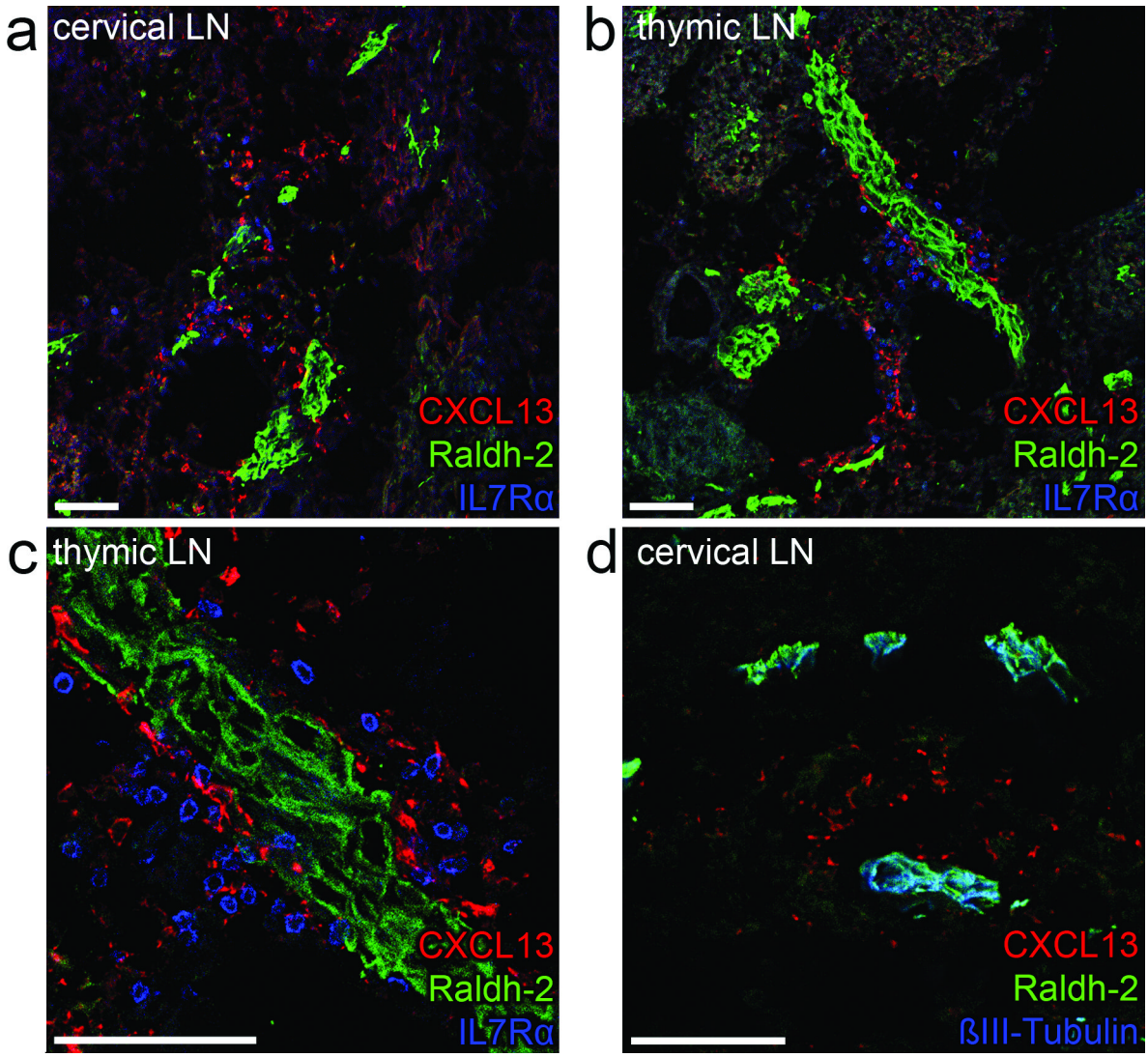

Figure 6. Raldh2 is localized in neurons adjacent to LN anlagen

E13.5 embryos (*n* = 8) were stained for Raldh1 and 2 in combination with CXCL13 (**a–c**) and neuronal marker anti-βIII-Tubulin (**d**). Shown are cervical (**a**) or peripheral thymic (**b**-detail in **c**) LN anlagen in which LTi cells are identified by IL7Rα. Bars represent 75 μm.

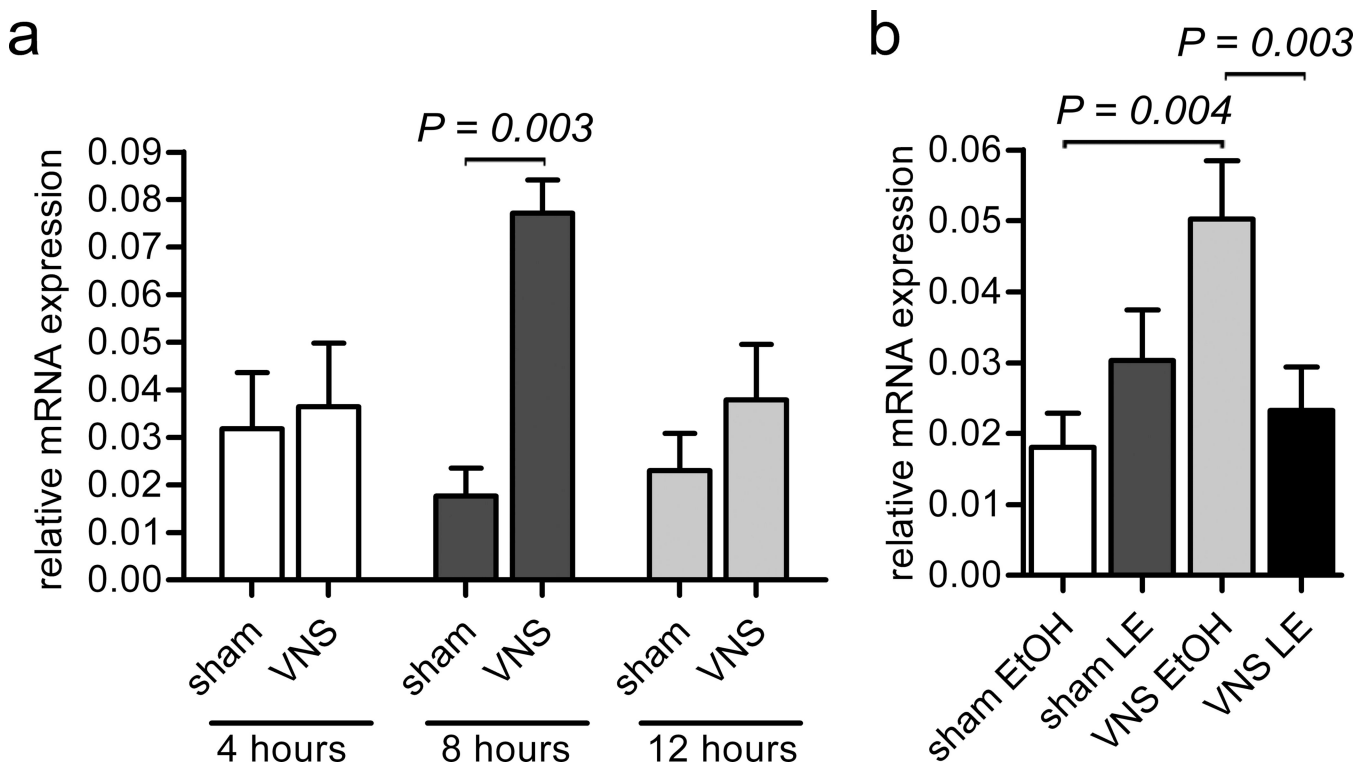

Figure 7. Stimulated neurons lead to CXCL13 expression

The right cervical vagal nerve was electrically stimulated (VNS) in adult mice and CXCL13 expression was analyzed in the ileum. As controls, animals were sham operated in which the vagal nerve was exposed, but not electrically stimulated (sham). (**a**) CXCL13 mRNA in the ileum at 4, 8, and 24 hrs after VNS (n = 3 independent experiments for each bar). (**b**) CXCL13 mRNA in the ileum at 8 hrs after VNS in the presence of injected RARβ blockers LE135 and LE540 (VNS LE) or vehicle (VNS ETOH) and in sham operated animals that received LE135 and LE1540 (sham LE) or vehicle alone (sham ETOH). (n = 6–9 independent experiments. Error bars represent the standard error.